Open Access

Journal of Energy and Power Technology

LIDSEN Publishing Inc.

Research Article

Harvesting the Potential of CO_2 before it is Injected into Geological Reservoirs

Tran X Phuoc *, Mehrdad Massoudi

National Energy Technology Laboratory (NETL), U.S. Department of Energy, P. O. Box 10940, 626 Cochrans Mill Road Pittsburgh, PA 15236, USA; E-Mails: Phuoc.Tran@netl.doe.gov; Mehrdad.Massoudi@netl.doe.gov

* **Correspondence:** Tran X Phuoc; E-Mail: Phuoc.Tran@netl.doe.gov

Academic Editor: Mohsen Abbaszadeh

Special Issue: Carbon Capture, Utilization and Storage: Challenges and Advances

Journal of Energy and Power Technology
2021, volume 3, issue 4
doi:10.21926/jept.2104050

Received: October 28, 2021
Accepted: December 19, 2021
Published: December 22, 2021

Abstract

To store CO_2 in geological reservoirs, expansion valves have been used to intentionally release supercritical CO_2 from high-pressure containers at a source point to lower-pressure pipelines and transport to a selected injection site. Using expansion valves, however, has some shortcomings: (i) the fluid potential, in the form of kinetic energy and pressure which can produce mechanical work or electricity, is wasted, and (ii) due to the Joule-Thomson cooling effect, the reduction in the temperature of the released CO_2 stream might be so dramatic that it can induce thermal contraction of the injection well causing fracture instability in the storage formation. To avoid these problems, it has been suggested that before injection, CO_2, should be heated to a temperature slightly higher than that of the reservoir. However, heating could increase the cost of CO_2 injection. This work explores the use of a Tesla Turbine, instead of an expansion valve, to harvest the potential of CO_2, in the form of its pressure and kinetics, to generate mechanical work when it is released from a high-pressure container to a lower-pressure transport pipeline. The goal is to avoid throttling losses and to produce useful power because of the expansion process. In addition, due to the friction between the gas and the turbine disks, the expanded gas temperature reduction is not as dramatic as in the case when

an expansion valve is used. Thus, as far as CO_2 injection is concerned, the need for preheating can be minimized.

Keywords
CO_2 sequestration; tesla turbine; geological reservoirs

1. Introduction

Expansion valves, including regulators, throttling valves, capillary tubes, etc., have been used to intentionally reduce the potential of a carrier fluid when it is delivered from a high-pressure container to the consumers or to the utilization sites at low specified pressure levels. In carbon capture and storage in formations beneath the earth surface, CO_2 generated from the main point source is stored in high-pressure containers. Expansion valves are usually used to release it to carrying pipelines with lower pressure for transporting it to a selected geological reservoir for long-term storage. Before injecting, CO_2 would need to be heated to a temperature slightly higher than that of the reservoir to avoid CO_2 condensation in the injection well and fracture instability in the storage formation [1-4]. Using expansion valves, however, has some shortcomings: (i) the fluid potential, in the form of kinetic energy and pressure, that can produce mechanical work or electricity, is wasted. In fact, a great deal of energy has been wasted due to all kinds of expansion valves that have been used to intentionally release and deliver natural gases from high-pressure lines to the consumers at lower specified pressure levels [5]. And (ii) the expanded CO_2 stream might be significantly cooled down due to the Joule-Thomson cooling effect. For CO_2 stored in a container of 40 ^oC and pressures of 25 to 15 MPa, the Joule-Thomson cooling effect could generate a decrease in the CO_2 temperature by 8 ^oC to 11 ^oC, respectively, as it expands to enter a transport pipeline of 8 MPa. Since CO_2 preheating consumes energy and expensive [6, 7], the Joule-Thomson cooling effect would dramatically increase the energy cost of injecting CO_2 in storage projects.

This work reports an exploratory study on the possibility of using a Tesla turbine, instead of a throttling/expansion valve, for releasing and delivering CO_2 from a high-pressure storage container to a transport pipeline at a lower pressure. Thus, the Joule-Thomson cooling effect is eliminated. Tesla turbines are simple, reliable, and bladeless (Figure 1). They are composed of flat, thin, and parallel co-rotating disks arranged normal to a shaft. When a working fluid is flowing through the gaps between the rotating disks, the shearing forces between the fluid and the rotating disks generate torques about the shaft producing mechanical work. Thus, when CO_2 is released through the gaps of a Tesla turbine, instead of an expansion valve, its potential, in the form of pressure, can be harvested to generate mechanical work. The novel concept of the present work is the use of a Tesla turbine as an alternative to a conventional expansion valve of any kind to avoid throttling losses and to produce useful power which can be used to generate electricity or to preheat CO_2 before injection. In addition, due to the friction between the gas and the turbine disks, the expanded gas temperature reduction is not as dramatic as is the case when an expansion valve is used. Thus, as far as CO_2 injection is concerned, the energy cost of injecting CO_2 can be minimized.

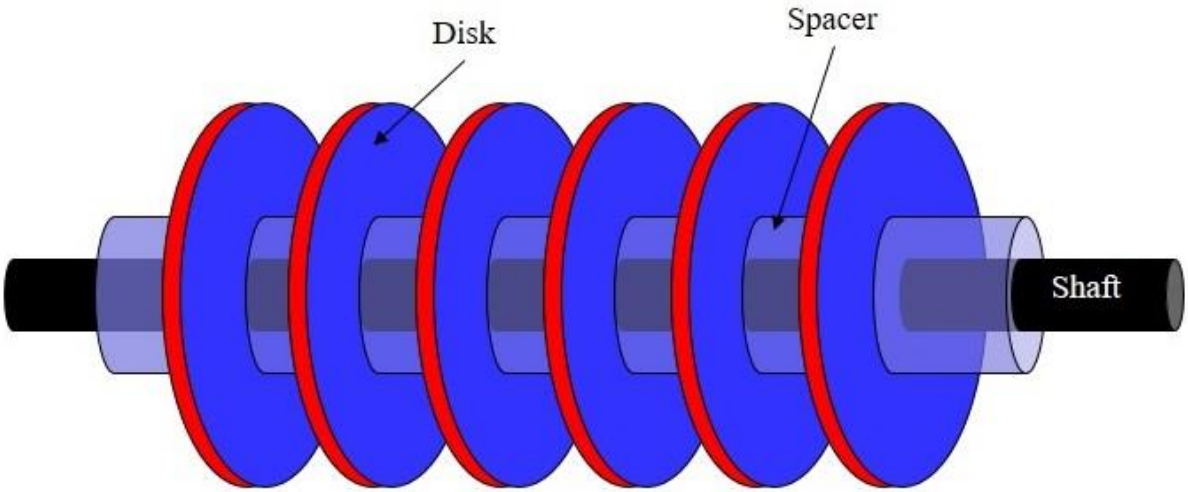

Figure 1 A schematic of a Tesla turbine.

In summary, the use of a Tesla turbine as a high-pressure CO_2 expansion device, its potential in the form of pressure and kinetics can be harvested to generate work and heat to preheat CO_2. Hence, characterizing the performance of a Tesla turbine using CO_2 as the working fluid is necessary. Tesla turbines have been investigated using air or water as the working fluid. Only in the last few years the Tesla turbine has been considered as a possible alternative to micro expanders for organic Rankine cycles [8, 9]. Song et al. [9] developed a code to assess the thermodynamic efficiency, as well as the power produced by a Tesla turbine working with different organic fluids. Aghagoli and Sorin [10] proposed a new transcritical carbon dioxide heat pump cycle, where a Tesla turbine was used to replace the expansion valve. They demonstrated that the coefficient of performance of the cycle is up to 16.3% higher than the traditional cycle with an expansion valve. In addition, when the rotor angular velocity is about 1000 rad/s, the turbine power is at its maximum; increasing the inlet pressure leads to the higher torque and consequently higher turbine power. At lower inlet pressure, the coefficient of performance of the heat pump cycle is higher. However, to the best of our knowledge, there are no studies investigating the use of a Tesla turbine as an integral component for CO_2 expansion, transport, and injection for long-term storage. Therefore, the main objective of this work is to estimate the Tesla turbine power output and its angular velocity when supercritical CO_2 of high pressure is released and delivered by a lower-pressure transport pipe. Such estimation will be carried out under a wide range of inlet and outlet pressures to show that as high-pressure CO_2 is released through a Tesla turbine, instead of a throttling/expansion valve, its potential to generate mechanical work is not wasted and can be harvested.

2. Simple Analysis

Conventional gas turbines expand the working fluid over the (aerodynamic) blades, producing a lift force on each blade that induces torque about the rotating drive shaft. A Tesla turbine relies on the fluid wall shear stress on the disks to convert the energy of the fluid to generate torque acting on the shaft. Figure 2 shows the release of supercritical CO_2 from a high-pressure container into a lower-pressure transport pipe via a Tesla turbine. As it is released, supercritical CO_2 enters the gap between the two rotating disks and exits the turbine after circulating about 360 degrees around the

shaft. While it flows between the disks, its momentum is reduced because part of it is used to generate torque to rotate the disks. Comprehensive assessment of Tesla turbine performance can be found in available literature [8, 11-13]. In these reports, the assessment was done through using the Navier-Stokes equations in cylindrical coordinates, under the assumptions of incompressible steady flow and neglecting the body forces.

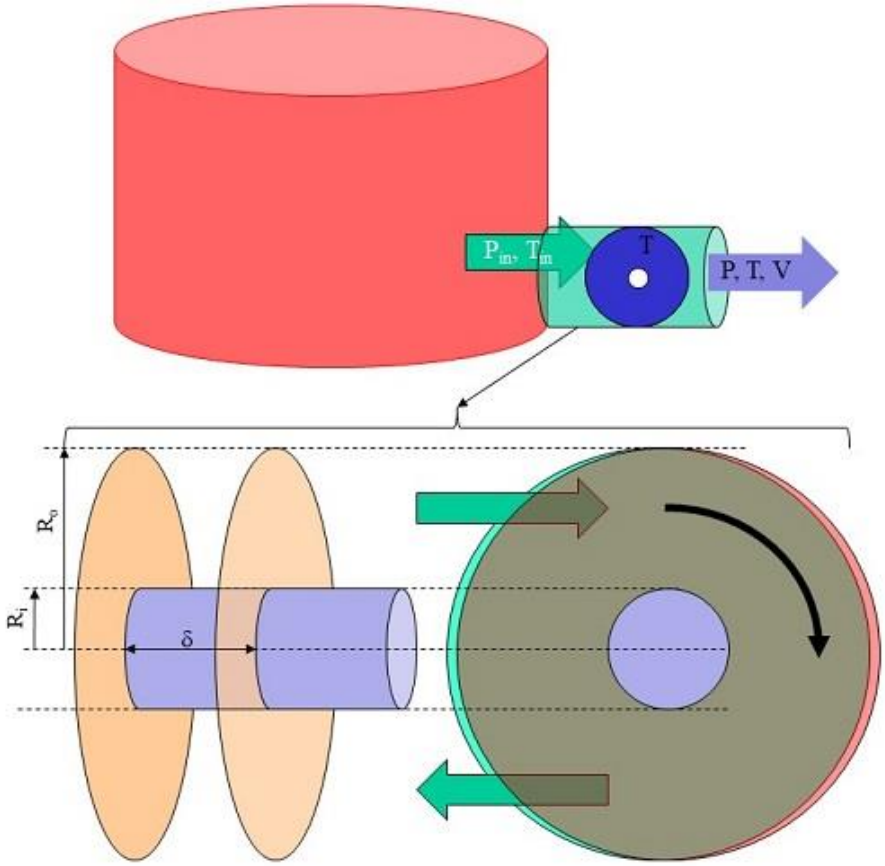

Figure 2 CO_2 released from a high-pressure container to a low-pressure transport pipe via a Tesla turbine; (P_{in} and T_{in} are the pressure and the temperature of CO_2 leaving the high pressure container and entering turbine. P, T, and V are the pressure, the temperature, and velocity of the CO_2 stream flowing through and leaving the turbine, T is the tesla turbine).

Tamir et al. [14] reported, both experimentally and analytically, a study on Tesla stall torques with air as the working fluid. By assuming laminar flow over a flat plate, an analytical model was developed where the turbine disk is divided into four separate pieces (one-quarter of the disk for each inlet port). Each piece has a length equal to a quarter of the disk's circumference, and a width equal to the difference between the outer and the inner disk radius. The shear force induced by the flow over these four separate pieces was assumed to be the shear induced by the laminar flow over a flat plate acting at the center of each plate. Comparing with the measured results, the model was seen to overpredict the measured Tesla turbine stall torques for inlet velocities up to 100 m/s, and under-predict the measured values for inlet velocities higher than 100 m/s. With considerations given to the uncertainties in the experimental data, the model predictions were in good agreement with the measured values, especially in the regime of high inlet flow velocities. In our present work,

we simply estimate the power harvested by CO_2 expansion using the pressure of the container, the pressure of the transport pipelines and the external torques as the parameters. Thus, this simple approach appears to be reasonable enough for the present calculations. The shear force induced by the flow is given as

$$F_t = 5.312U^{3/2}R_o^{3/2}\left(1-\frac{R_i}{R_o}\right)\sqrt{\frac{\pi\rho\mu}{4}\left(1+\frac{R_i}{R_o}\right)} \quad (1)$$

Where R_i and R_o are the rotating disk inner and outer radius, respectively, U is the velocity of CO_2 flowing through the gap between the disks, ρ and μ are the CO_2 density and viscosity respectively, and the linear velocity U is

$$U = V - V_D = V - R_o\omega \quad (2)$$

Where V (m/s) is the velocity of CO_2 flowing through the gap and V_D (m/s) and ω (rad/s) are the tangential and the angular velocities of the rotating disks, respectively. The resulting torque, τ_{strs}, is calculated by multiplying the shear forces by a lever arm equal to the distance from the disk's center to half the disk's width

$$\tau_{strs} = 10.624U^{3/2}R_o^{5/2}\left(1-\frac{R_i}{R_o}\right)\left(1+\frac{R_i}{R_o}\right)\sqrt{\frac{\pi\rho\mu}{4}\left(1+\frac{R_i}{R_o}\right)} \quad (3)$$

And the power, P_w (W), is calculated as

$$P_w = \tau_{strs}\omega \quad (4)$$

The power per unit mass, p_w (J/kg) is.

$$p_w = \frac{P_w}{\dot{m}} = \frac{P_w}{(R_o - R_i)\delta\rho_{CO_2}} \quad (5)$$

Where $\dot{m} = (R_o - R_i)\delta\rho_{CO_2}$ is the CO_2 mass flow rate, δ is the space between the rotors.

2.1 Turbine Angular Velocity, ω (rad/s)

As the working fluid enters and flows through the gap between the stationary disks, a velocity gradient near the disk is developed; this is responsible for the generation of the shear stress which in turn develops a torque, τ_{strs}, on the disk. When the turbine is not loaded, the resisting torque is the frictional torque of the shaft. If the torque developed by the shear stress is greater than the frictional torque, τ_{fr}, the disk will start rotating. If the turbine is loaded, the resisting torque is now due to the load, τ_{load}, and the frictional torque, τ_{fr}. With the resistant torque $\tau_r = \tau_{fr} + \tau_{load}$, the angular speed is calculated as

$$\tau_{strs} - \tau_r = I\frac{d\omega}{dt} \quad (6)$$

Where I is the moment of inertia of the rotating disks. With the disk thickness β, each channel has two rotating disks, and if the turbine density is ρ_t, then the turbine mass is approximated as the mass of the channel $m = 2\pi\rho_t R_o^2\beta$; thus, the moment of inertia I is

$$I = \frac{mR_o^2}{2} = \pi\rho_t R_o^4\beta \tag{7}$$

With Eqn. (7), the angular speed is determined as

$$\frac{d\omega}{dt} = \frac{(\tau_{strs} - \tau_r)}{\pi\rho_t R_o^4\beta} \tag{8}$$

2.2 Calculating the Fluid Velocity V

The velocity of CO_2 at the turbine inlet is assumed to be zero. However, the velocity of CO_2 as it passes through the turbine is not negligible. Referring to Figure 2, the momentum conservation across the turbine can be written as

$$Momentum: P_1 - \frac{F_t}{A_t} = P + \rho V^2 \tag{9}$$

The CO_2 velocity entering the rotors is calculated from Eqn. (9) as

$$V = \left(\frac{P_1 - \frac{F_t}{A_t} - P}{\rho} \right)^{1/2} \tag{10}$$

Where A_t is the cross sectional area of the gap. With δ as the gap space, A_t is approximated as

$$A_t = (R_o - R_i)\delta \tag{11}$$

2.3 Thermophysical Properties of CO_2

Fundamental equations for calculating the thermodynamic properties of CO_2 have been reported in literature [15-17]. These equations were expressed in terms of the dimensionless Helmholtz free energy (A/RT) which depends on density and temperature and they are applicable for the temperature range from the Triple-Point to 1100 K and pressures up to 800 MPa. For the transport properties, the correlations developed by Vesovic et al [18] and Fenghour et al. [19] for the transport properties of CO_2 are used in our analysis. We then compare the results with those obtained from NIST database [20]. It was found that the average deviation is about 0.2% for CO_2 density and less than 0.1% for all other properties.

3. Results and Discussions

In this section we will present our results for the estimated turbine output power using the analytical equations presented in Section 2; the power output is a function of the external torques, the pressures of the container and of the transport pipelines. For a given load, the performance of

a Tesla turbine depends on the geometric parameters of the turbine (for example, the main geometric parameters are the ratio between the inlet and the outlet disk radius, the external diameter of the space between the disks, the thickness of the disks, etc.) and the operating conditions (inlet/outlet pressures, inlet/outlet temperatures). The turbine material influences its angular speed as shown by Eqn. (8). The heat transfer between the fluid and the turbine can affect the CO_2 exhaust temperature as mentioned in the introduction. Thus, both turbine material and heat transfer might have some effects on the numerical values of the calculated output power. Their roles, however, on the manner by which the output power can depend on the external torques, the pressures of the container and the transport pipelines are insignificant. Therefore, in this work, we did not include the heat transfer effect and we only looked at the effects of the operating conditions while the turbine geometric parameters as well as its material were kept unchanged. The operating conditions here are mainly the pressures and the temperatures of the high-pressure container and of the transport pipelines. Since CO_2 remains supercritical for the conditions of pressure and temperature of many geological reservoirs, its state during the injection process must be supercritical. Thus, the pressures in the transport pipelines are chosen from 8 to 12 MPa and the pressures of the high-pressure container are from 15 MPa to 25 MPa.

In a Tesla turbine, as the fluid enters at a high velocity, a velocity gradient near the disks is developed, generating the shear stress which in turn develops the torque, τ_{strs}, on the disks. When the turbine is not loaded the resisting torque is the frictional torque of the shaft. If the torque developed by the shear stress is greater than the frictional torque, τ_{fr}, the disk will start rotating. As the disk rotating speed increases, the relative velocity of the fluid with respect to the disk, (Eqn. (2)), decreases and so is the shear stress causing the torque. Eventually, the torque due to the shear stress is balanced by the frictional torque and a steady-state condition is reached; the disk is rotating at a constant angular velocity. For the same inlet/outlet conditions, if the turbine is loaded, the resisting torque is due to the load and the frictional torques, and the rotational speed at steady state will be less than that of the steady rotational speed at no load. Thus, using steady-state condition, the performance of a Tesla turbine in terms of its angular velocity and the power output under various load conditions are determined.

Examples of such steady-state conditions are shown in Figure 3, Figure 4 and Figure 5. Figure 3 shows the results on the angular velocity, ω, and the relative velocity, U, as a function of time due to the effect of the external loads while the inlet pressure and the outlet pressure are kept constant at 20 MPa and 8 MPa, respectively. The results indicate that for a given load, the angular velocity increases rapidly and levels off to a constant value after a short time. The values of the angular velocity are seen to increase as the load decreases. For example, when the load is 0.1 N-m, the angular velocity increases rapidly and reaches the steady state condition at 2382 rad/s after about 3 s. When the load is 2.5 N-m, the steady state condition is reached just after 2.1 s and the angular velocity is 278 rad/s. The effects of the external load on the relative velocity U as a function of time can be seen from Figure 3(b). For a fixed condition of the inlet and the outlet pressures, the magnitude of the relative velocity at steady state increases with the external load. In the range of the external loads and the operational pressures reported here, the relative velocity of about 180 m/s is achievable with the external load of 2.5 N-m when the operating condition is kept at 25 MPa inlet pressure and 8 MP outlet pressure.

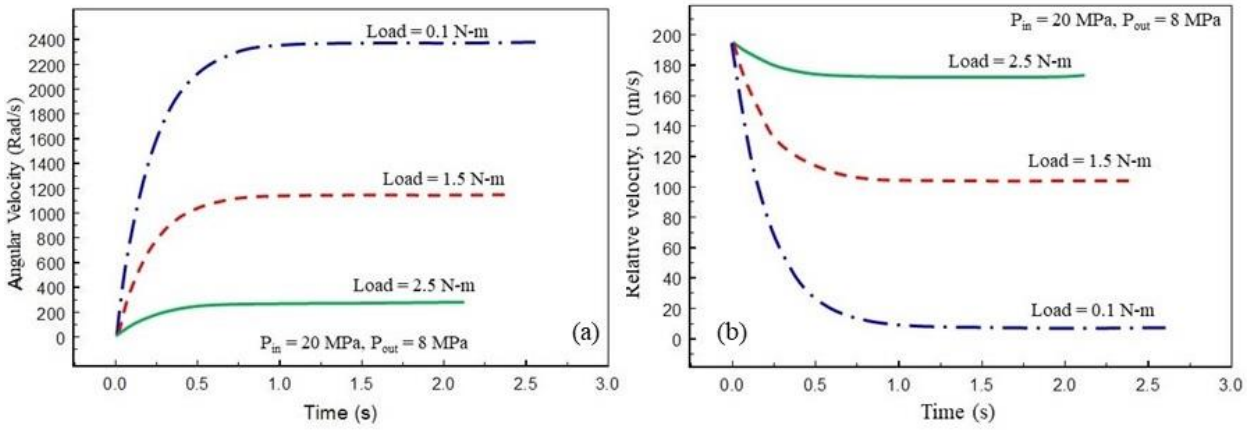

Figure 3 (a) Angular velocity, ω, and (b) the relative Velocity, U, as a function of time. The effect of the load, (Inlet pressure = 20 MPa; Outlet pressure = 8 MPa; T_0 = 311 K, R_i = 40 mm, R_o = 80 mm, gap, δ = 0.8 mm, disk thickness, β = 0.8 mm, and the turbine density, ρ_t = 2500 kg/m^3).

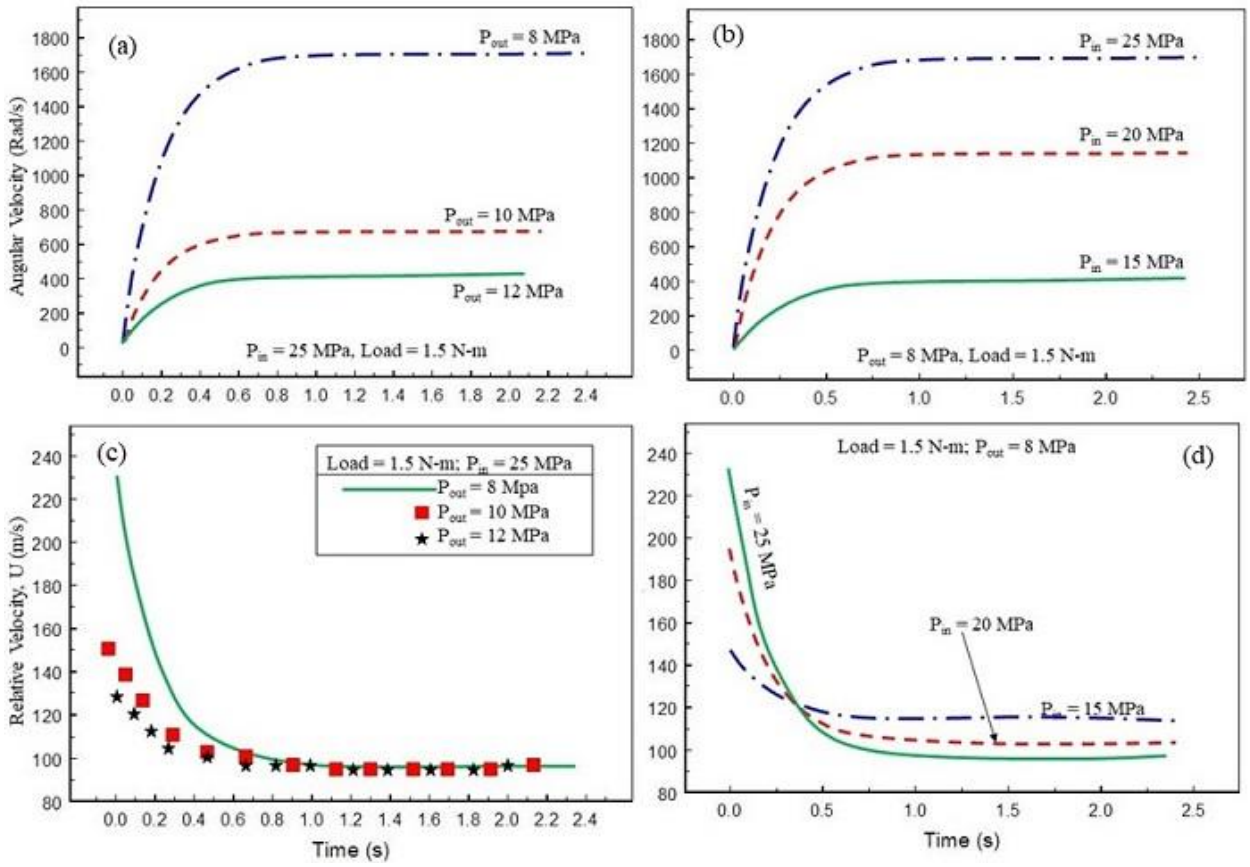

Figure 4 Angular velocity and the relative velocity as a function of time: (a) Effect of the outlet pressure, (b) effect of inlet pressure; (typical conditions: T_0 = 311 K, τ_{load}= 1.5 N-m, R_i = 40 mm, R_o = 80 mm, gap, δ = 0.8 mm, disk thickness, β = 0.8 mm, and the turbine density, ρ_t = 2500 kg/m^3).

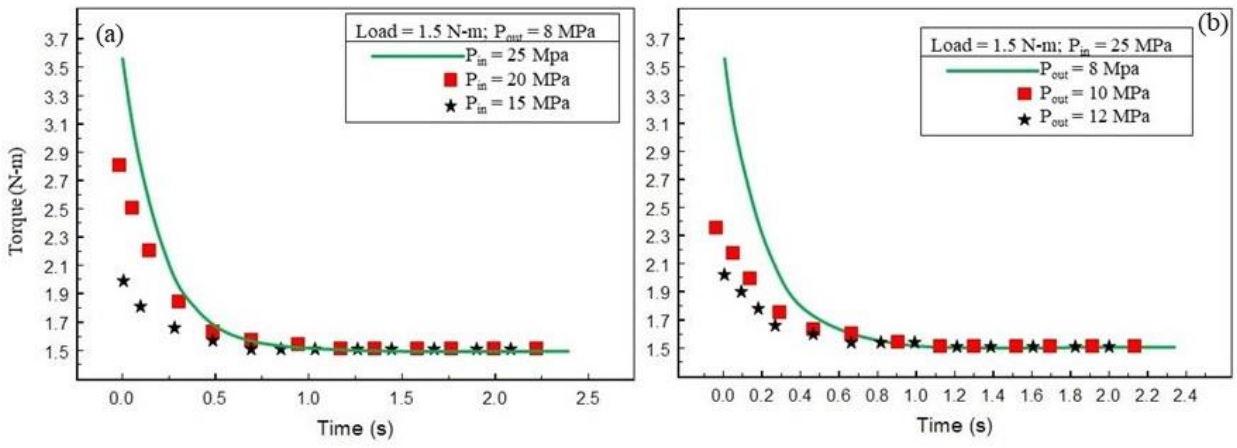

Figure 5 Torque as a function of time, (a) the effect of the inlet pressure and (b) the effect of the outlet pressure (Load = 1.5 N-m, T_0 = 311 K, R_i = 40 mm, R_o = 80 mm, gap, δ = 0.8 mm, disk thickness, β = 0.8 mm, and the turbine density, ρ_t = 2500 kg/m^3).

For a fixed external load, the angular velocity increases with the inlet pressure but decreases as the outlet pressure increases as shown in Figure 4 where results on the angular velocity and the relative velocity as a function of time under different operating conditions when the external load is kept constant at 1.5 N-m are presented. For the case with the inlet pressure of 25 MPa, the angular velocity levels off to 1715 rad/s after 2.36 s when the outlet pressure is 8 MPa and it decreases to 437 rad/s after 2.09 s when the outlet pressure increases to 12 MPa. Figure 4(b) shows the results when the outlet pressure is kept at 8 MPa and the inlet pressures are 15, 20, and 25 MPa. The turbine reaches a constant angular velocity of 427 rad/s in 2.42 s and to 1715 rad/s in 2.36 s as the inlet pressure increases from 15 MPa to 25 MPa. The effects of the inlet pressures and the outlet pressures on the relative velocity U as a function of time are shown in Figure 4(c) and Figure 4(d). The results indicate that, for a given external load, the relative velocity is independent of the outlet pressure when the inlet pressure is kept constant, but it decreases as the inlet pressure increases if the outlet pressure is kept unchanged. The decrease in the relative velocity at higher inlet pressures is due to the fact that the momentum transfer between the working fluid and the rotating disks depends on both the relative velocity and the fluid density and viscosity. Since both the fluid density and its viscosity are higher at higher pressures, the relative velocity must be lower for the torque to be balanced by the same external load.

The effects of the inlet pressures and the outlet pressures on the torque due to the shear stress as a function of time are shown in Figure 5. The results indicate that as the steady state condition is reached, all the torques level off at the external load, independent of the operating conditions in terms of the inlet and the outlet pressures. The operating conditions, however, determine the initial value of the torque and hence they determine the maximum external load that the turbine is operational. Figure 6 shows the effects of the operating condition in terms of the inlet and the outlet pressures on the steady-state torque as a function of the eternal loads. Using supercritical CO_2 as the working fluid, the range of the external loads that a turbine can be operated is seen to increase with higher inlet pressures and lower outlet pressures. For example, for the outlet pressure of 8 MPa, the turbine can operate with an external load of 1.7 N-m at the inlet pressure of 15 MPa and with an external load up to 3.2 N-m when the inlet pressure is up to 25 MPa. For a constant inlet pressure at 20 MPa, the turbine with the outlet pressure of about 8 MPa can operate with an

external load of 2.5 N-m while with an outlet pressure of 12 MPa the external load is up to 1.3 N-m. The increase of the torque with the external load, shown in Figure 6, can be explained in terms of the turbine angular velocity. This is shown in Figure 7 where the angular and the relative velocities as a function of the external load are presented. As the load increases, the angular velocity decreases, and the relative velocity increases. Since the working fluid transfers more momentum to the disks at higher relative velocity as shown by Eqn. (1), a higher torque is developed.

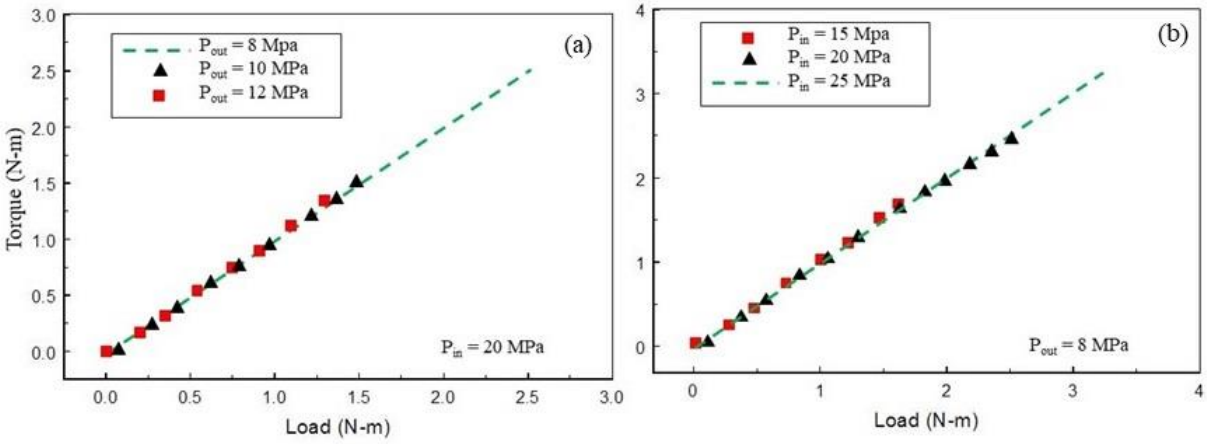

Figure 6 Torque as a function of load, (a) the effect of the outlet pressure and (b) the effect of the inlet pressure (T_0 = 311 K, R_i = 40 mm, R_o = 80 mm, gap, δ = 0.8 mm, disk thickness, β = 0.8 mm, and the turbine density, ρ_t = 2500 kg/m^3).

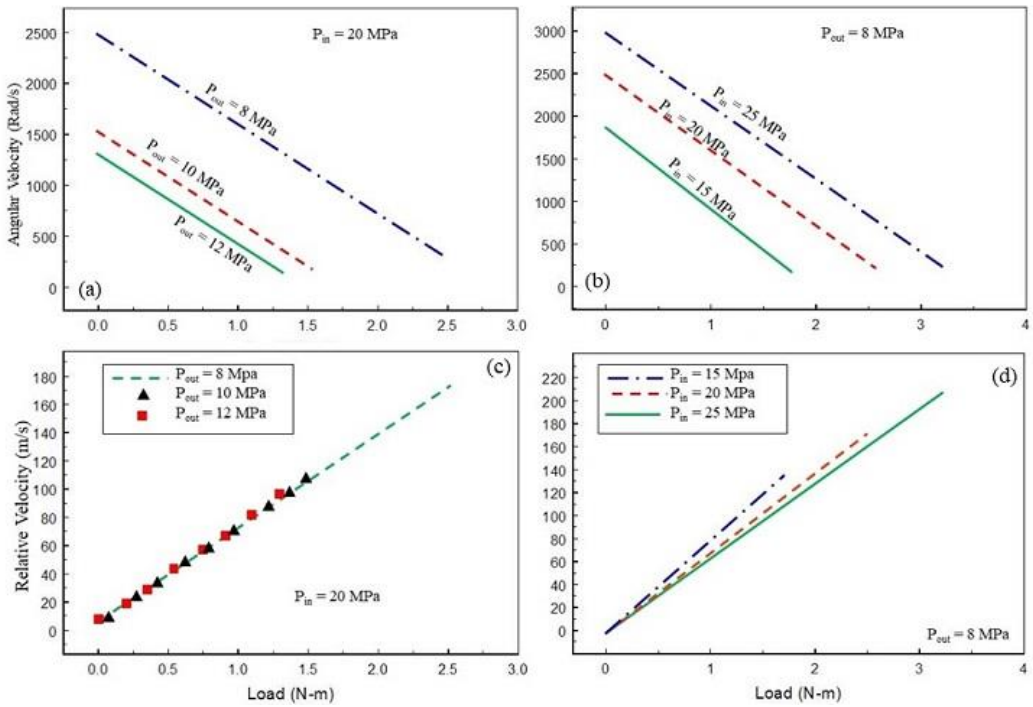

Figure 7 Angular velocity and the relative velocity as a function of load, Figures a and c: the effect of the outlet pressure; Figures b and d: the effect of the inlet pressure; (T_0 = 311 K, R_i = 40 mm, R_o = 80 mm, gap, δ = 0.8 mm, disk thickness, β = 0.8 mm, and the turbine density, ρ_t = 2500 kg/m^3).

Figure 8 shows the effects of the inlet and the outlet pressures on the outlet power as a function of the external loads. The operational range of the external load increases as either the inlet pressure increases, or as the outlet pressure decreases. The power outlet depends on the inlet and the outlet enthalpies and the kinetic energies; it can be calculated using Eq. 4, $P_w = \tau\omega$, which describes the increase of the power outlet as the angular velocity increases. Increasing the angular velocity results in a decrease of the relative velocity reducing the momentum transfer from the fluid to the disks and hence, increasing the outlet velocity. Increasing the outlet velocity, however, has a negative effect on the power output of the turbine. Thus, since the angular velocity depends on the operational torque, increasing/decreasing the operational load has both positive and negative effects on the power output. At first, the turbine power increases with the increase in the external load until a maximum point and then the turbine power decreases as the load continues to increase. For a fixed inlet pressure, both the maximum point and the operational range of the external loads decrease as the outlet pressure increases. For a fixed outlet pressure, the maximum point and the operational range of the external loads increase as the inlet pressure increases. Operating with supercritical CO_2 as the working fluid, when the inlet pressure is 20 MPa, the maximum power output of 1739 W and the angular velocity of about 1241 rad/s are obtained at the external load of 1.4 N-m for the outlet pressure of 8 MPa, and the inlet pressure of 20 MPa. The range of the operational external load is up to 2.5 N-m. For the outlet pressure of 8 MPa, the operational range of the external load is up to 3.1 N-m, the maximum power of 2646 W occurs at the external load of 1.8 N-m (1469 rad/s) for the inlet pressure of 25 MPa. This power is calculated for one channel. For a turbine having 100 channels, a power output of 0.2646 MW could be harvested instead of being wasted if conventional throttling expansion valves of any kinds are used. To roughly estimate the energy required to increase the temperature of CO_2 transported in an 8 MPa pipeline, we use the following equation $\dot{Q} = \dot{m}_{CO2} c_{p,CO2} \Delta T$. If this power is used to preheat the transported CO_2 to increase its temperature by 10 °C, ($\Delta T = 10$), before injection, it is sufficient to heat an amount 0.8 Mt of CO_2 per year. Goodarzi et al. [7] estimated the cost of heating to avoid cooling the reservoir to be about $0.75 per cubic meter; thus, a heating cost of about a million dollars per year would be saved.

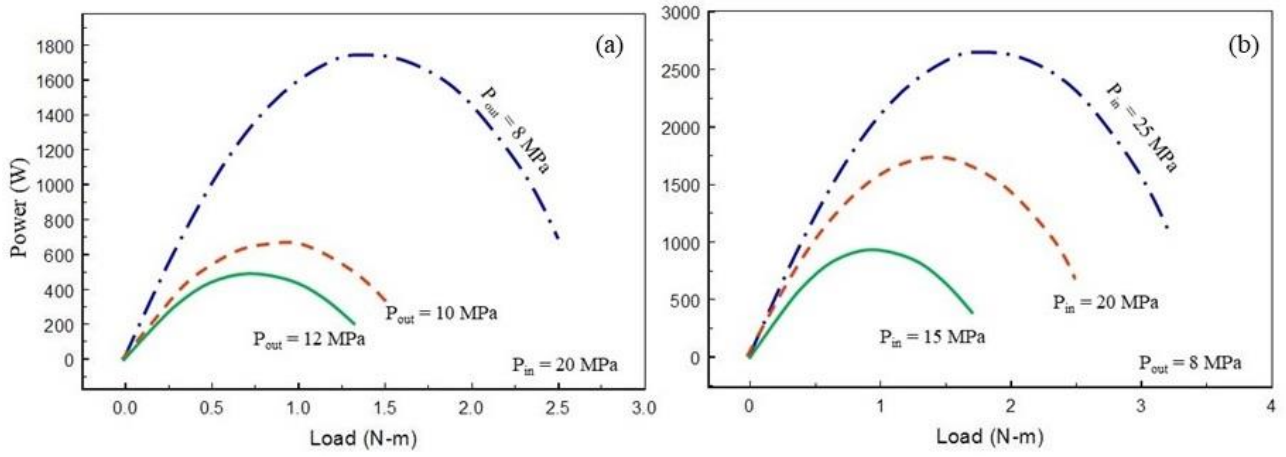

Figure 8 Power outlet as a function of load; (a): the effect of the outlet pressure, (b): the effect of the inlet pressure; (T_0 = 311 K, friction torque, R_i = 40 mm, R_o = 80 mm, gap, δ = 0.8 mm, disk thickness, β = 0.8 mm, and the turbine density, ρ_t = 2500 kg/m^3).

4. Conclusion

This study presents a simple analysis to look at the performance of a Tesla turbine, in terms of its angular velocity and power, while using supercritical CO_2 as the working fluid. The work is based on the simple analytical model developed by Tamir et al. [14]. Keeping the turbine geometric parameters unchanged, while the inlet temperature, the inlet pressures, and the outlet pressures are used as the operating conditions. The results show that using a Tesla turbine instead of a conventional expansion valve of any kinds, to expand and deliver supercritical CO_2 from a high-pressure container to a lower-pressure transport pipelines, throttling losses can be avoided and its potential to generate useful mechanical work can be harvested. In addition, due to the friction between the expanded CO_2 and the turbine disks, its temperature reduction is not as dramatic as is the case when an expansion valve is used. Thus, as far as CO_2 injection is concerned, the need for preheating can be minimized.

Disclaimer

"This report was prepared as an account of work sponsored by an agency of the United States Government. Neither the United States Government nor any agency thereof, nor any of their employees, makes any warranty, express or implied, or assumes any legal liability or responsibility for the accuracy, completeness, or usefulness of any information, apparatus, product, or process disclosed, or represents that its use would not infringe privately owned rights. Reference herein to any specific commercial product, process, or service by trade name, trademark, manufacturer, or otherwise does not necessarily constitute or imply its endorsement, recommendation, or favoring by the United States Government or any agency thereof. The views and opinions of authors expressed herein do not necessarily state or reflect those of the United States Government or any agency thereof."

Author Contributions

Phuoc X. Tran thought of this problem and performed most of the derivations and all of the calculations. Mehrdad Massoudi helped in the derivation and the formulation of the problem. Both authors contributed to the writing of the paper, and both authors have read and agreed to the published version of the manuscript.

Competing Interests

The authors have declared that no competing interests exist.

References

1. Teodoriu C. Why and when does casing fail in geothermal wells: A surprising question? Proceedings of the world geothermal congress 2015; 2015 April 19th-25th; Melbourne, Australia. Berlin: ResearchGate.
2. Kaldal GS, Jónsson MÞ, Pálsson H, Karlsdóttir SN. Structural analysis of casings in high temperature geothermal wells in Iceland. Proceedings of the world geothermal congress 2015; 2015 April 19th-25th; Melbourne, Australia. Berlin: ResearchGate.

3. Roy P, Walsh SD, Morris JP, Iyer J, Hao Y, Carroll S, et al. Studying the impact of thermal cycling on wellbore integrity during CO_2 injection. Proceedings of the 50th U.S. Rock Mechanics/Geomechanics Symposium; 2016 June 26th-29th; Houston, Texas, USA. Richardson: OnePetro.
4. Liebscher A, Möller F, Bannach A, Köhler S, Wiebach J, Schmidt-Hattenberger C, et al. Injection operation and operational pressure-temperature monitoring at the CO_2 storage pilot site Ketzin, Germany-design, results, recommendations. Int J Greenh Gas Control. 2013; 15: 163-173.
5. Sheikhnejad Y, Simões J, Martins N. Energy harvesting by a novel substitution for expansion valves: Special focus on city gate stations of high-pressure natural gas pipelines. Energies. 2020; 13: 956.
6. Möller F, Liebscher A, Martens S, Schmidt-Hattenberger C, Streibel M. Injection of CO_2 at ambient temperature conditions-pressure and temperature results of the "cold injection" experiment at the Ketzin pilot site. Energy Procedia. 2014; 63: 6289-6297.
7. Goodarzi S, Settari A, Zoback MD, Keith DW. Optimization of a CO_2 storage project based on thermal, geomechanical and induced fracturing effects. J Pet Sci Eng. 2015; 134: 49-59.
8. Fiaschi D, Talluri L. Design and off-design analysis of a Tesla turbine utilizing CO_2 as working fluid. In: E3S Web of Conferences. Les Ulis: EDP Sciences; 2019. pp.03008.
9. Song J, Ren XD, Li XS, Gu CW, Zhang MM. One-dimensional model analysis and performance assessment of Tesla turbine. Appl Therm Eng. 2018; 134: 546-554.
10. Aghagoli A, Sorin M. CFD modelling and exergy analysis of a heat pump cycle with Tesla turbine using CO_2 as a working fluid. Appl Therm Eng. 2020; 178: 115587.
11. Manfrida G, Talluri L. Fluid dynamics assessment of the Tesla turbine rotor. Therm Sci. 2019; 23: 1-10.
12. Talluri L, Fiaschi D, Neri G, Ciappi L. Design and optimization of a Tesla turbine for ORC applications. Appl Energy. 2018; 226: 300-319.
13. Ciappi L, Fiaschi D, Niknam PH, Talluri L. Computational investigation of the flow inside a Tesla turbine rotor. Energy. 2019; 173: 207-217.
14. Emran TA, Alexander RC, Stallings CT, DeMay MA, Traum MJ. Method to accurately estimate Tesla turbine stall torque for dynamometer or generator load selection. Proceedings of the 2010 ASME Early Career Technical Conference; 2010 October 1st-2nd; Atlanta, Georgia, USA. New York: The American Society of Mechanical Engineers.
15. Span R, Wagner W. A new equation of state for carbon dioxide covering the fluid region from the triple-point temperature to 1100 K at pressures up to 800 MPa. J Phys Chem Ref Data. 1996; 25: 1509-1596.
16. Span R, Wagner W. Equations of state for technical applications. III. Results for polar fluids. Int J Thermophys. 2003; 24: 111-162.
17. Kim Y. Equation of state for carbon dioxide. J Mech Sci Technol. 2007; 21: 799-803.
18. Vesovic V, Wakeham WA, Olchowy GA, Sengers JV, Watson JT, Millat J. The transport properties of carbon dioxide. J Phys Chem Ref Data. 1990; 19: 763-808.
19. Fenghour A, Wakeham WA, Vesovic V. The viscosity of carbon dioxide. J Phys Chem Ref Data. 1998; 27: 31-44.

20. National Institute of Standards and Technology. NIST chemistry webbook [Internet]. Gaithersburg: National Institute of Standards and Technology. Available from: http://webbook.Nist.Gov/.

Enjoy *JEPT* by:

1. Submitting a manuscript
2. Joining in volunteer reviewer bank
3. Joining Editorial Board
4. Guest editing a special issue

For more details, please visit:
http://www.lidsen.com/journal/jept